

Purified Compound of the Seeds of *Carica Papaya* Loaded mPEG-PLA Polymeric Nanomicelle (MCPI-PNs) for Reproductive Studies in Albino Male Rats

Abdul S. Ansari*, Rajeev Kumar Dhaked, Barkha Khilwani and Nirmal K. Lohiya

Centre for Advanced Studies, Department of Zoology, University of Rajasthan, Jaipur, Rajasthan 302004, India

(*) Corresponding author: abdulsansari@yahoo.com
(Received: 23 August 2023 and Accepted: 06 May 2024)

Abstract

This study compares the characterized MCP I-loaded methoxy poly (ethylene glycol)-poly (lactic acid) polymeric nanomicelles (MCPI-PNs) of different sizes and doses to find out the maximum antireproductive effects with purified compound of seeds of *Carica papaya*. The prepared MCPI-PNs consisting of six groups ($n=36$), viz., vehicle treated control (group 1), alone MCP I @ 10 mg/animal/day (group 2), 46.03 nm sized blank mPEG-PLA nanomicelles @ 0.3 mL/animal/day (group 3), 100 nm sized MCPI-PNs (1.5, 3.0 and 4.5 $\mu\text{g}/\text{animal}/\text{day}$) (group 4), 129 nm sized MCPI-PNs (4.5, 9.0 and 13.5 $\mu\text{g}/\text{animal}/\text{day}$) (group 5) and 166 nm sized MCPI-PNs (13.5, 27.0 and 45.0 $\mu\text{g}/\text{animal}/\text{day}$) (group 6) were orally treated for a period of 30 days in albino male rats. Animals of groups 2, 4, 5 and 6 showed significantly altered sperm parameters. However, the sperm concentration maximally dropped in group 2 and 4 (low dose and mid dose), respectively, indicating the range of oligozoospermia to severe oligozoospermia in these groups. The fertility declined to zero percent in groups 2 and 4 (low dose), whereas all animals were 100% fertile in rest of groups. Histopathological studies of testes exhibited sloughing and eruption of germ cells with inhibition of spermatogenesis in groups 2 and 4, whilst some conspicuous alterations in spermatogenesis was observed in groups 5 and 6 when compared to groups 1 and 3. Based on the above observations, the group 4 (100 nm sized MCPI-PNs) at low dose regimen (1.5 $\mu\text{g}/\text{animal}/\text{day}$) exhibited maximum antifertility effects in male albino rats.

Keywords: Drug delivery systems, mPEG-PLA polymeric nanomicelles, MCPI-PNs, Reproductive effects, Male albino rats.

1. INTRODUCTION

The seed extracts of *Carica papaya* have shown promise in male contraception. Preliminary investigation in rats and rabbits with different extracts/fractions of the seeds and variable dose, duration and mode of administration, revealed maximum anti-fertility with the chloroform extract [1,2]. Further purification of the product revealed maximum activity was found in the benzene chromatographic fraction of the chloroform extract in rats and rabbits [3,4] without any toxicity [5]. The methanol and ethyl acetate sub-fractions of the benzene chromatographic fraction also showed sperm motility inhibition in rats following 30–60 days of

treatment and azoospermia in rabbits within 15 days of treatment [2, 6]. The benzene fraction yielded two principal components each from the methanol sub-fraction (MCP I, II) and the ethyl acetate sub-fraction (ECP I, II) [7]. The MCP I exerted systemic action on the sperm parameters and sperm immobilizing effects on human spermatozoa *in vitro* [6-8].

Macromolecules in the past several decades have developed into a very useful class of drug delivery system (DDS) [9-12]. However, their therapeutic applications are not always successful due to lack of sustained, controlled and targeted delivery resulted into poor efficacy of

active drugs to the target sites [13]. Thus, a suitable DDS is required that controls the release of drugs and possesses higher efficiency. In this direction, several drug delivery systems (DDSs), such as metal nanoparticles, liposomes, dendrimers polymeric nanomicelles and nanotubes [14-19], have attracted a lot of interest due to easy preparation, good biocompatibility and high efficiency [20]. The polymeric nanomicelle systems have advantages over other DDSs due to their amphiphilic nature for encapsulation of non-water-soluble agents in their hydrophobic core [21-24]. We prepared polyethylene glycol–polylactic acid (mPEG-PLA) copolymer/polymer micelle DDS of which chemical and biological properties have been well documented [25]. However, the role of mPEG-PLA polymeric nanomicelles as a potential DDS in reproductive studies has not yet been carried out, so far. Therefore, in the present investigation a comparative account on different sizes of the mPEG-PLA nanomicelles, namely MCP I loaded polymeric nanomicelles (MCPI-PNs), with already established purified compound of *Carica papaya* (MCP I) as a male contraceptive, on male reproductive system and general toxicity have been made in albino rats.

2. MATERIALS AND METHODS

Test Material

Fresh seeds of *Carica papaya* L. (Caricaceae) of honey dew variety (Voucher No. RUBL 16590 at the Department of Botany, University of Rajasthan, Jaipur, India) was procured from local supplier, powdered and subjected to chloroform extraction. The obtained extract was then processed on silica gel column chromatography for benzene fraction. The benzene fraction was further sub-fractionated and the active compound MCP I was obtained from methanol sub-fraction as reported earlier [7].

Chemicals

Poly (ethylene glycol) methyl ether (mPEG), D, L-lactide and stannous octoate were obtained from Sigma Aldrich Chemical Pvt. Ltd, (Bangalore, India). Dichloromethane and diethyl ether were purchased from Merck Specialities Pvt. Ltd. (Mumbai, India). All other chemicals were of analytical grade and used as received.

Animals

Clinically healthy, adult male Wistar albino rats (*Rattus norvegicus*) weighing 140-180 g and 5-6 months old were used. Animals were maintained in the Departmental experimental animal facility with 12:12 hrs light and dark schedule in polypropylene cages (size 43 x 27 x 15 cm). Animals were fed with rat pellet diet (Ashirwad Industries Limited, Chandigarh) and free access to water. The temperature in animal house was maintained at 25 ± 2 °C. Experiments were conducted in compliance with the Guidelines on the Regulation of Scientific Experiments on Animals [26]. The experiment protocol was approved by the Institutional Animal Ethics Committee (IAEC).

2.1. Synthesis of Polyethylene Glycol–Polylactic acid (PEG-PLA) Copolymer/Polymer

The polyethylene glycol–polylactic acid (PEG-PLA) copolymer/polymer was synthesized by ring opening polymerization method [27] with certain modifications. In brief, in a dried round bottomed flask 10 g of mPEG (Mw=5000 Da) was heated at 130 °C in an oil bath to eliminate the water content then 1 g of D, L-lactide, and 4 mL of toluene were added by continuous stirring with a magnetic stirring bar. After that, the mixture was again heated (130 °C) with continuous stirring and 1 mL of stannous octoate as catalyst was added for polymerization process for a period of 22-24 h. The polymerization process was terminated by adding 0.1 N methanolic KOH. The

recrystallization process was carried out by addition of dichloromethane and then precipitated via diethyl ether as co-solvent at -20 °C. The residual solvent was removed from the purified PEG-PLA copolymer/polymer by drying in a desiccator fitted with a vacuum evaporator at room temperature for a period of 24-48 h.

2.2. Preparation of Blank mPEG-PLA and MCP I Loaded (MCPI-PNs) Nanomicelles

The blank mPEG-PLA nanomicelles were synthesized by direct dissolution method [27]. Briefly, into a round bottomed flask the synthesized 0.40 mg of mPEG-PLA copolymer was added in 1 mL of Milli-Q water with continuous agitation on a magnetic stirrer for a period of 30 min. at room temperature. Due to the amphiphilic properties, the mPEG-PLA copolymer self-assembled into micelles. After blank mPEG-PLA micelles were obtained, again four separate sets of round bottomed flasks were taken and the measured quantity of 5 μ L, 15 μ L and 45 μ L of MCP I was loaded into mPEG-PLA micelles for preparation of copolymeric/polymeric nanomicelles (MCPI-PNs) for a period of 30 min. at room temperature then the suspension was filtered by a 220 nm pore size syringe filter (Millex-GP, Merck Specialities Pvt. Ltd. (Mumbai, India) to remove the free MCP I. Finally, the blank PNPs and MCPI-PNs nanomicelles were used for further application.

2.3. Determination of the Physico-chemical Properties of Prepared mPEG-PLA and MCPI-PNs

The ^1H -Nuclear Magnetic Resonance Spectroscopy (NMR) analysis of the polymer was performed using NMR spectrometer ECS 400 MHz (JEOL, Tokyo, Japan) supplied with a new generation 5 mm tunable broad band gradient probe. Deuterated dimethylsulphoxide (DMSO-d_6) and trimethylsilane (TMS), respectively, used as solvent and

internal standard for baseline corrections. Proton (^1H) spectra (400 MHz) were recorded with pulse duration of 30 second, a recycle delay of 2.0 second and 16 scans [28].

The synthesized mPEG-PLA copolymer/polymer was carried out for Fourier transform infrared spectroscopy (FTIR) analysis [29]. The FTIR spectra were recorded at room temperature (from 4000-400 cm^{-1} with 16 scanned) using FTIR Spectrum 2 (Perkin Elmer, New York, USA).

The synthesized mPEG-PLA copolymer was carried out for X-ray diffraction (XRD) measurement using the X-Ray diffractometer (Panalytical X'Pert Pro, Almelo, the Netherlands) with $\text{CuK}\alpha$ radiation ($\lambda = 1.542 \text{ \AA}$) operated at 30 kV and 30 mA. Data were recorded in 2θ range of 2° – 10° at the scan rate of $2^\circ/\text{min}$ [30].

The mean diameter (zeta potential), polydispersity index (PDI) and intercept unit were determined by dynamic light scattering (DLS) on a Zetasizer 300 HS instrument (Malvern Instrument Ltd., UK) at room temperature [31]. All results were the mean of 3 test runs.

The morphology of mPEG-PLA and MCPI-PNs was studied under a scanning electron microscope (Nova Nano FE-SEM 450; FEI) at an accelerating voltage of 15 kV [32]. A thin film of polymeric nanomicelles was smeared on a clean glass slide, air dried, mounted on SEM stub and sputter coated with a thin layer of gold (10 nm) prior to observation.

Samples for transmission electron microscopic (TEM) observation were prepared by placing a drop of sample solution on to a carbon coated copper grid (mesh size 200). Excess solution was wiped away with filter paper. The grid was further stained with phosphotungstic acid (2% w/w) and allowed to dry [33]. The samples were examined using the Tecnai G2 20 S-Twin (FEI) at 200 kV accelerating voltage.

2.4. Experimental Protocol

Three prepared MCPI-PNs (sizes 100 nm, 129 nm and 166 nm) were orally treated, containing 3 animals for a dose regimen of each nanomicelle (three dose regimens of every prepared nanomicelles) for a period of 30 days. Animals were divided into following groups:

Group 1: Animals (vehicle treated control) were treated with olive oil (0.3 mL/animal/day; oral) for a period of 30 days (n=3)

Group 2: Animals were treated with MCP I (10 mg/animal/day; oral) for a period of 30 days (n=3)

Group 3: Animals were treated with 46.03 nm sized blank PNs (0.3 mL/animal/day; oral) for a period of 30 days (n=3)

Group 4: Animals were treated with low (L), mid (M) and high (H) doses of 100 nm sized MCPI-PNs (1.5, 3.0 and 4.5 µg/animal/day; oral) for a period of 30 days [n=9 (3x3)]

Group 5: Animals were treated with low (L), mid (M) and high doses (H) of 129 nm sized MCPI-PNs (4.5, 9.0 and 13.5 µg/animal/day; oral) for a period of 30 days [n=9 (3x3)]

Group 6: Animals were treated with low (L), mid (M) and high doses (H) of 166 nm sized MCPI-PNs (13.5, 27.0 and 45.0 µg/animal/day; oral) for a period of 30 days [n=9 (3x3)]

The required doses were suspended in olive oil (0.3 mL) and the drug was orally fed with the help of a feeding needle fitted in a graduated syringe. Due care was taken to ensure that the complete dose received by animals. All animals from each group were sacrificed with a subcutaneous overdose of thiopentone sodium (Thiosol sodium, Neon Laboratories Ltd., Mumbai) at 30 days test period, after collecting the body weight and completing fertility test. Upon sacrifice, reproductive organ weights were measured. The separated testes for histopathology and cauda epididymides for sperm characteristics were processed.

PARAMETERS

Body Weight and Organs Weight

The initial and final body weights of experimental animals were recorded. Reproductive organs (testes, epididymides, vas deferens, seminal vesicle and ventral prostate) were dissected out, freed from fat and adherent tissues and weighed at the nearest milligram on an electronic balance.

Cauda Epididymal Sperm Characteristics

The cauda epididymis (100 mg) was finely fragmented in 1 mL of normal physiological saline, and the clear fluid was used for analyses of sperm concentration, motility, viability and abnormality [34].

Fertility Test

Rats were subjected to fertility test following 30 days of drug administration with proven fertile female rats at 1:2 ratio. Success of mating was confirmed by appearance of vaginal plug and presence of spermatozoa in the vaginal smear. Thereafter, the females were caged separately and kept under observation till confirmation of pregnancy. Fifty percent of the pregnant animals were allowed to complete the term and the pregnancy record was maintained. The remaining females were sacrificed at 3rd week of gestation for teratological observations.

Histopathology of Testes

Testis was fixed in 4% paraformaldehyde, dehydrated in various grades of ethanol, cleared in xylene, infiltrated and embedded in paraffin wax. Sections of 5 µm thickness were cut and stained with hematoxylin and eosin for observation under light microscope.

Statistical Analysis

The values were represented as mean ± standard deviation (SD) and one way analysis of variance (ANOVA) was applied for statistical comparison using

SPSS (version 10.0) software. Statistical significance was determined at a value of $p < 0.05$.

3. RESULTS

Characterization of mPEG-PLA Copolymer/ Polymer and mPEG-PLA Nanomicelles

The $^1\text{H-NMR}$ results showed peaks at 1.19, 4.53 and 5.35 ppm were assigned methyl (A), methyne (C) and hydroxyl (D) protons of poly (D,L-Lactide) (PLA) repeating unit and the peak at 4.12 (B) ppm were attributed to the protons of mPEG adjacent of $-\text{COO}$ of PLA end group. The peak at 3.28 (E) ppm was attributed $-\text{CH}_2-\text{CH}_2-$ group of mPEG repeating unit. The NMR results indicated the synthesis of mPEG-PLA copolymer/polymer (Fig. 1A).

Coupling reaction was characterized with FTIR analysis. Fig. 1B shows the IR spectra of mPEG-PLA copolymer/polymer. For PLA, the band at 3427 cm^{-1} was corresponding to O-H stretching vibration of end group and the bands at 2885 cm^{-1} due to the C-H stretching vibration of asymmetric $-\text{CH}_3$ (Vas CH_3) group. The peak at 1746 cm^{-1} assigned to the stretching vibration of carboxylic group and peak at 1631 cm^{-1} stretching vibration of ester carbonyl group. The peak at 1468 cm^{-1} and $1358, 1344\text{ cm}^{-1}$ C-H stretching scissoring of symmetric CH_2 and asymmetric CH_3 groups. Peak at 1281 cm^{-1} C-O stretching scissoring of asymmetric C-O-C group and peak at $1146, 1110\text{ cm}^{-1}$ C-O stretching vibration of C-O-C group of PLA and peak at 1061 cm^{-1} C-O stretching vibration of C-O group of PLA. The peak at $960, 842\text{ cm}^{-1}$ assigned to the stretching vibration of CH_2-CH_2 group and peak at $600, 529\text{ cm}^{-1}$ the stretching vibration of CH_3 end group of mPEG. The FTIR analysis result shows that mPEG unit attached to PLA unit to form a linear structure of mPEG-PLA copolymer and polymer.

The PNs analysis by FTIR indicated the peak at 3308 cm^{-1} due to stretching vibration of O-H group of water, peak at

1631 cm^{-1} showed stretching vibration of ester carbonyl group of PLA and peak at 585 cm^{-1} was CH stretching of CH-CH group of mPEG.

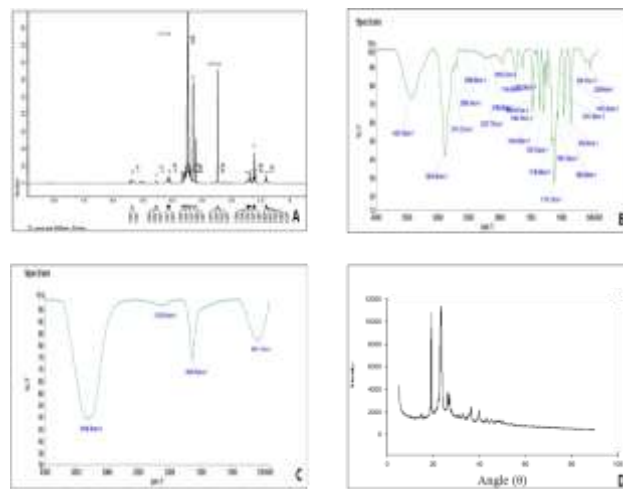


Figure 1. Characterization of mPEG-PLA copolymer/ polymer and PNs. (a) $^1\text{H-NMR}$ spectrum of mPEG-PLA copolymer/polymer, (b) IR spectra of mPEG-PLA copolymer/ polymer, (c) IR spectra of PNs and (d) XRD pattern of mPEG-PLA copolymer/polymer.

Formation of PNs did not alter bonds present in copolymer/polymer (Fig. 1C). The XRD patterns obtained from the mPEG-PLA copolymer are shown in the Fig. 1D. The diffraction pattern of the mPEG-PLA indicates that a broad amorphous peak of PLA was observed around 19.23° . This confirms the PLA has an amorphous microstructure. By adding of more mPEG, the intensity of the diffraction peak becomes stronger, confirming the increased crystallization in mPEG-PLA at 23.34° . It indicates the crystalline structure of mPEG-PLA was slightly increased by formation of copolymer.

Characterization of MCPI-PNs

The average size (d. nm), polydispersity index (PDI) and intercept unit of blank PNs was 46.03 nm , 0.263 and 0.920 , respectively. The average size (d. nm), polydispersity index (PDI)

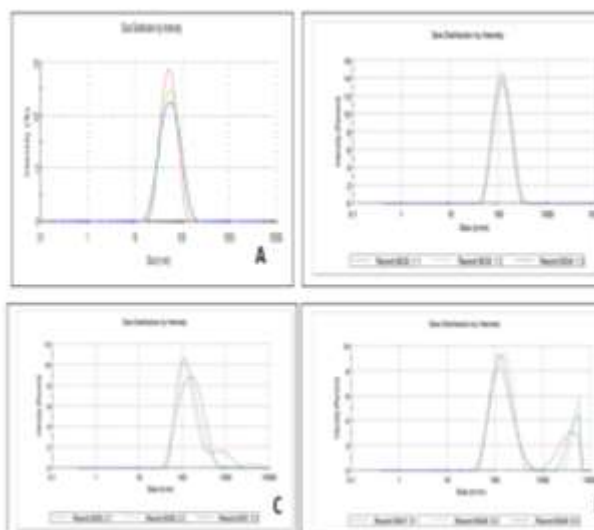


Figure 2. Characterization of PN and MCPI-PNs. DLS images: (A) Blank PN 46.03 nm, different sizes MCPI-PNs (B) 100 nm, (C) 129 nm, and (D) 166 nm.

Table 1. Dynamic light scattering (DLS) data of blank mPEG-PLA and MCPI-PNs nanomicelles.

MCP I (µg)	Z-average (nm)	Polydispersity index (PDI)	Intercept unit
0	46.03	0.263	0.874
5	100	0.145	0.915
15	129	0.254	0.916
35	154	0.469	0.891
45	166	0.532	0.877

and intercept unit of 5 µg MCP I filled MCPI-PNs was found to be 100 nm, 0.145 and 0.915, respectively. The addition of more amount of MCP I in PNs enhanced the average size (d. nm) of MCPI-PNs. When 15 µg and 45 µg of MCP I added, accordingly the reported average sizes (d. nm) of MCPI-PNs, respectively, were 129 nm and 166 nm. The respective PDI and intercept unit of these MCPI-PNs, respectively, were 0.254 and 0.916, and 0.532 and 0.877 (Fig. 2A-D, Table 1).

The SEM morphology of blank mPEG-PLA exhibited smooth contour and spherical shape with diameters ranged 20 to 70 nm. While, the MCPI-PNs also indicated smooth surface and spherical morphology with higher diameters from 50 to 100 nm (Fig. 3A-B).

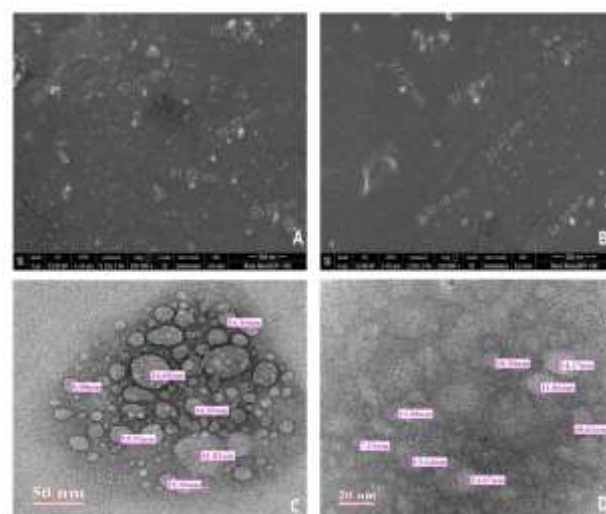


Figure 3. Characterization of PN and MCPI-PNs. SEM images of Blank blank PNs (A) and MCPI-PNs (B) and TEM image of Blank PNs (C) and MCPI-PNs (D).

The TEM of blank and MCPI-PNs also showed monodispersed and spherical shape with varied diameters ranged 20 to 100 nm (Fig. 3C-D).

Body and Reproductive Organs Weight

The body weights of animals of all experimental groups (2 - 6) remain unaltered when compared with group 1 (vehicle treated control) animals throughout the study period (data not shown). The reproductive organs weight of all experimental groups (2-6) did not exhibit any remarkable changes as compared to vehicle treated control (group 1) animals (Table 2).

Cauda Epididymal Sperm Characteristics

The cauda epididymal sperm characteristics indicated a reduction in sperm concentration which was found to be drastically significant ($p \leq 0.001$) in groups 2, 4, 5 and 6 following treatments when compared to vehicle treated control (group 1). However, the sperm concentration maximally dropped in group 2 (10 mg/animal/day), group 4 (low dose and mid doses).

Table 2. Cauda epididymal sperm characteristics following treatment with MCP I alone, blank mPEG-PLA and MCPI-PNs in dose finding study for a period of 30 days in male albino rats.

Groups	Doses	Sperm Concentration (Million/mL)	Sperm Motility (%)	Sperm Viability (%)	Sperm Abnormality (%)
Group 1 (Vehicle treated control)	0.5 mL/animal/day	82.33±1.62	84.25±0.61	86.57±1.38	16.90±0.67
Group 2 (MCP I alone)	10 mg/animal/day (Low dose)	16.13±1.73*	5.00±1.63*	6.28±1.54*	78.50±0.15*
Group 3 (Blank mPEG-PLA)	0.3 mL/animal/day (Low dose)	72.47±8.82	78.33±6.24	84.16±1.63	17.66±0.09
	0.6 mL/animal/day (Mid dose)	73.58±3.39	79.33±4.19	79.00±0.82	18.71±0.05
	0.9 mL/animal/day (High dose)	76.42±1.36	80.67±3.09	80.42±1.58	17.64±0.09
Group 4 (100 nm sized MCPI-PNs)	1.5 µg/animal/day (Low dose)	2.58±0.13*	5.33±2.05*	7.67±2.05*	90.54±0.14*
	3 µg/animal/day (Mid dose)	6.80±1.83*	8.33±1.25*	10.33±0.94*	88.21±0.06*
	4.5 µg/animal/day (High dose)	10.22±0.90*	13.08±1.53*	14.83±1.84*	85.58±0.11*
Group 5 (129 nm sized MCPI-PNs)	4.5 µg/animal/day (Low dose)	48.99±7.03*	15.08±3.44*	59.83±6.86*	80.42±0.11*
	9.0 µg/animal/day (Mid dose)	47.69±1.94*	25.33±11.59*	28.42±10.29*	75.57±0.08*
	13.5 µg/animal/day (High dose)	33.50±1.95*	12.75±2.07*	14.75±2.07*	70.45±0.10*
Group 6 (166 nm sized MCPI-PNs)	13.5 µg/animal/day (Low dose)	48.96±5.90*	16.67±2.87*	18.42±2.52*	71.32±0.04*
	27.0 µg/animal/day (Mid dose)	39.70±4.54*	16.42±1.23*	17.42±1.23*	65.54±0.13*
	40.5 µg/animal/day (High dose)	39.08±6.57*	20.33±2.05*	21.75±1.14*	66.48±0.10*

*Statistically significant ($p \leq 0.001$) when compared with group 1 (vehicle treated control); Values are expressed as mean±S.D. (n=3)

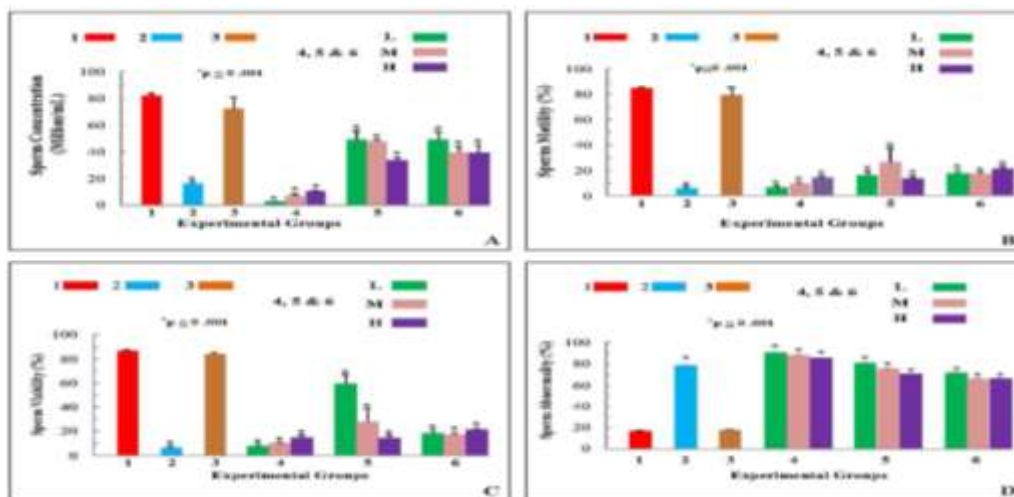


Figure 4. Cauda epididymal sperm characteristics following treatment with MCP I, PNs and MCP I-PNs for a period of 30 days in male albino rats. (A) Cauda epididymal sperm concentration in different groups. Note variable reduction in sperm counts. (B) Drastic reduction of sperm motility in different groups. (C) Sperm viability indicates low values in different groups and (D) An enhancement in the sperm abnormalities in different groups.

In groups 2, 4, 5 and 6, the sperm motility and viability exhibited a drastic reduction ($p \leq 0.001$) following treatment. A

significant enhancement in the sperm abnormality was noticed following

treatment in groups 2, 4, 5 and 6 ($p \leq 0.001$) (Fig. 4A-D).

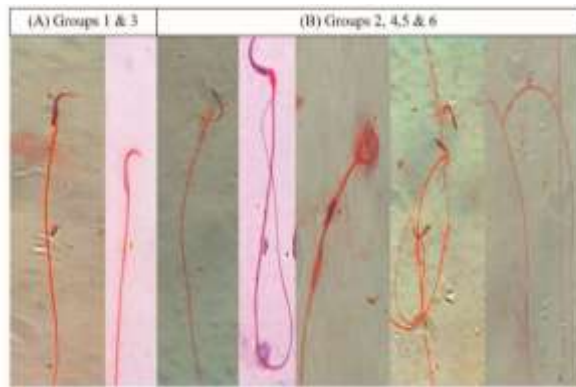


Figure 5. Morphology of cauda epididymal spermatozoa. (A) Groups 1 and 3 showing normal configuration. (B) Various abnormalities were detected in spermatozoa of different experimental groups (2, 4, 5 and 6) during treatment with MCP I and MCPI-PNs for a period of 30 days in male albino rats. X 1000.

Morphology of Cauda Epididymal Spermatozoa

The spermatozoa in groups 1 and 3 animal depicted typical hook shaped head and long tail. The acrosome of head showed smooth configuration with thick plasma membrane. Acrosome and post-acrosomal regions were prominent. Neck piece was also prominent, characterized by its distinct constriction. The mid-piece was long, thick and separated with the tail piece along with well-defined distinction, the annuli. The tail piece was long and cylinder ended with an abrupt narrowing. In groups 2, 4, 5 and 6 animals, various degrees of abnormalities such as head-tail separation, acrosomal damage, bent mid-piece and coiled tail was seen following treatment (Fig. 5).

Histopathology of Testes

Group 1: The testis of group 1 (vehicle treated control) animals showed round or oval seminiferous tubules containing Sertoli cells and germ cells of various stages covering the complete

spermatogenesis. Thin lamina propria showing closer association with spermatogonia and Sertoli cells were seen. Spermatogonia were oval in shape, resting on the basement membrane. Germ cell differentiation appeared normal and the spermatocytes and spermatids were prominent with well-defined nuclei and distinct cytoplasm. The Sertoli cells depicted with typical irregular nuclei and granular cytoplasm and also had closer association with germ cells and the elongated spermatids. The lumen contained abundant spermatozoa. The interstitium occupied with intertubular elements and distinct Leydig cells containing round, granular and prominent nuclei (Fig. 6A).

Group 2: In group 2 (MCP I @10 mg/animal/day), the testes exhibited disruption of spermatogenesis in most of the tubules. Germ cells differentiation beyond spermatocytes was sparsely seen. Vacuolization in the Sertoli cells was seen. Lumen contained numerous erupted germ cells. The interstitium contained fibroblast like cells. The Leydig cell nuclei appeared to be normal (Fig. 6B).

Group 3: Group 3 (blank PNs @0.3 mL/animal/day) animals showed testicular features alike with that of the group I animals. In brief, round or oval seminiferous tubules with the epithelium containing Sertoli cells and germ cells with various spermatogenic stages were seen. The lumen filled with numerous spermatozoa. Normal Leydig cells were present in the interstitium (Fig. 6C).

Group 4: In group 4 animals treated with low (1.5 $\mu\text{g}/\text{animal}/\text{day}$), mid (3.0 $\mu\text{g}/\text{animal}/\text{day}$) and high (4.5 $\mu\text{g}/\text{animal}/\text{day}$) doses of 100 nm sized MCPI-PNs, exhibited inhibition of spermatogenesis mostly at spermatid stage. Seminiferous tubules filled with masses of eosinophilic material were noted. Germ cells appeared to be pycnotic. Eruption of germ cells was appeared in most of the seminiferous tubules. The vacuolization of the Sertoli cells was seen. The fibroblast

like cells in the interstitium with normal Leydig cells was present. The effects were more or less similar in all three dose regimens (Figs. 6D-F).

Group 5: In group 5 animals treated with low (4.5 $\mu\text{g}/\text{animal}/\text{day}$), mid (9.0 $\mu\text{g}/\text{animal}/\text{day}$) and high (13.5 $\mu\text{g}/\text{animal}/\text{day}$) doses of 129 nm sized MCPI-PNs, were present with inhibition of

spermatogenesis in some seminiferous tubules. Erupted immature germ cells were seen in the lumen. All stages of spermatogenesis were found in majority of tubules. The vacuolization in Sertoli cells were seen in these tubules. Normal Leydig cell nuclei with intertubular elements were noticed.

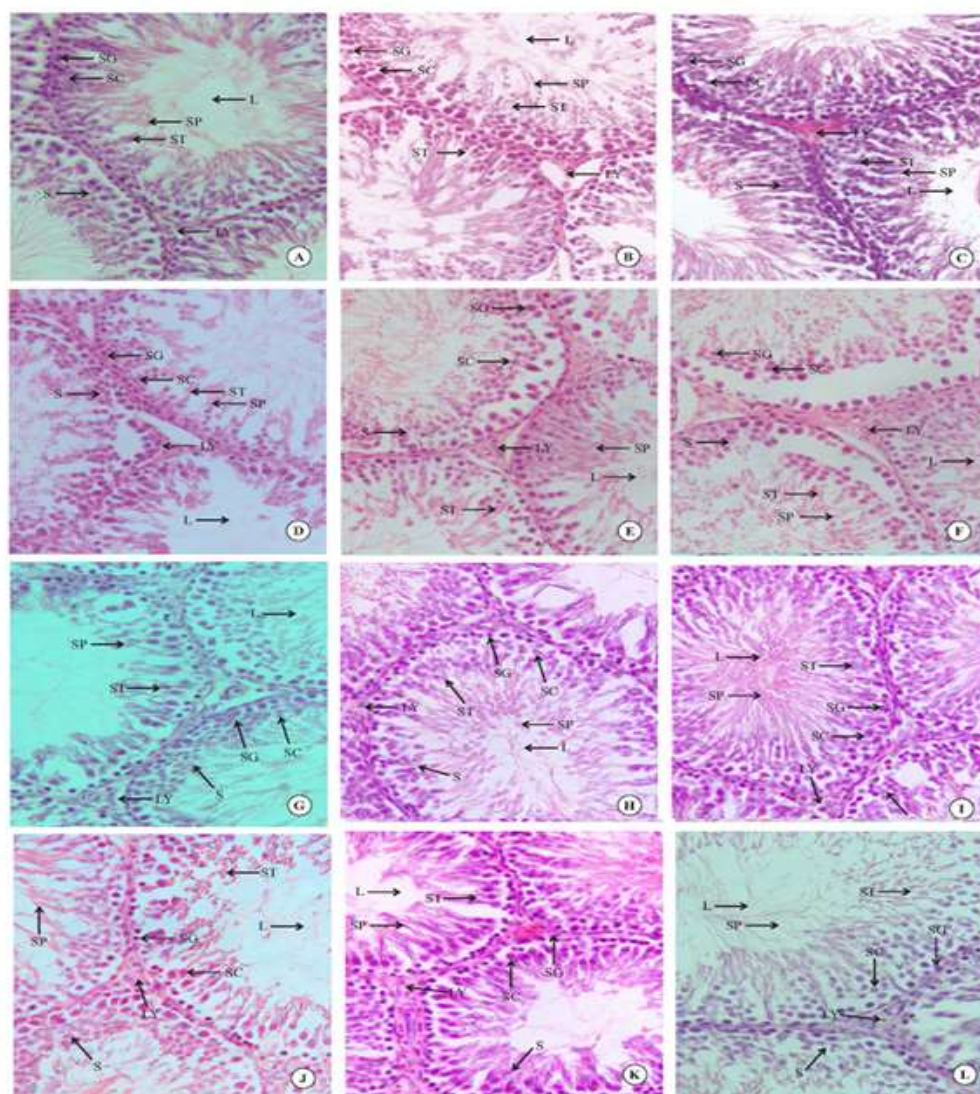


Figure 6. Histopathology of testis following oral treatment for a period of 30 days in Wistar rats: (A) group 1 (vehicle treated control); (B) group 2 (MCP I @ 10 mg/animal/day); (C) group 3 (46.3 nm sized blank PNs @ 0.3 mL/animal/day); (D-F) group 4 [100 nm sized MCPI-PNs @ low dose (1.5 $\mu\text{g}/\text{animal}/\text{day}$), mid dose (3.0 $\mu\text{g}/\text{animal}/\text{day}$) and high dose (4.5 $\mu\text{g}/\text{animal}/\text{day}$)]; (G-I) group 5 [129 nm sized MCPI-PNs @ low dose (4.5 $\mu\text{g}/\text{animal}/\text{day}$), mid dose (9.0 $\mu\text{g}/\text{animal}/\text{day}$) and high dose (13.5 $\mu\text{g}/\text{animal}/\text{day}$)] and (J-L) group 6 [166 nm sized MCPI-PNs @ low dose (13.5 $\mu\text{g}/\text{animal}/\text{day}$), mid dose (27.0 $\mu\text{g}/\text{animal}/\text{day}$) and high dose (45.0 $\mu\text{g}/\text{animal}/\text{day}$)]. SG: Spermatogonia, SC: Spermatocytes, S: Sertoli Cells, ST: Spermatid, SP: Spermatozoa L: Lumen, LY: Leydig Cells.

All three dose regimens showed similar effects (Figs. 6 G-I).

Group 6: In group 6 animals treated with low (13.5 µg/animal/day), mid (27.0 µg/animal/day) and high (@40.5 µg/animal/day) doses of 166 nm sized MCPI-PNs exhibited active spermatogenesis in most of the tubules. Few seminiferous tubules possessing inhibition of spermatogenesis also showed with vacuolization of Sertoli cells. Lumen contained few erupted germ cells. The diameter of the seminiferous tubules was

unaltered. The Leydig cells were found to be normal along with intertubular elements in the interstitium. All three dose regimens exhibited more or less similar testicular features (Figs. 6 J-L).

Fertility Test

In groups 2 and 4, zero fertility was evident only at low dose regimens. In remaining groups and their respective dose regimens, animals showed cent percent fertility at 30 days of mating schedule (Table 3).

Table 3. Fertility record following treatment with MCP I alone, blank mPEG-PLA and MCPI-PNs in dose finding study for a period of 30 days in male albino rats.

Groups	Doses	No. of males mated with females in 1:2 ratio	No. of males showed confirmed fertility	% fertility
Group 1 (Vehicle treated control)	0.5 mL/animal/day (Low dose)	3	3/3	100
Group 2 (MCP I alone)	10 mg/animal/day	3	0/3	0
Group 3 (Blank mPEG-PLA)	0.3 mL/animal/day (Low dose)	3	3/3	100
	0.6 mL/animal/day (Mid dose)	3	3/3	100
	0.9 mL/animal/day (High dose)	3	3/3	100
Group 4 (100 nm sized MCPI-PNs)	1.5 µg/animal/day (Low dose)	3	0/3	0
	3 µg/animal/day (Mid dose)	3	3/3	100
	4.5 µg/animal/day (High dose)	3	3/3	100
Group 5 (129 nm sized MCPI-PNs)	4.5 µg/animal/day (Low dose)	3	3/3	100
	9.0 µg/animal/day (Mid dose)	3	3/3	100
	13.5 µg/animal/day (High dose)	3	3/3	100
Group 6 (166 nm sized MCPI-PNs)	13.5 µg/animal/day (Low dose)	3	3/3	100
	27.0 µg/animal/day (Mid dose)	3	3/3	100
	40.5 µg/animal/day (High dose)	3	3/3	100

Values are expressed as mean±S.D. (n=3)

4. DISCUSSION

Polymeric nanomicelle mediated drug delivery allows prolonged, localized and target-specific interaction of the drug with the targeted organ. Development of

nanotechnology-based DDSs improves therapeutic index of the drug by effective administration and enhancing the exposure to target sites. Also, the polymeric nanomicelles provide an effective way to

improve drug solubilization, develop clear aqueous formulations and deliver drugs to target tissues. The amphiphilic nature of nanomicelles encapsulates hydrophobic drugs that enhance drug delivery. Drug loaded nanomicelles also effectively enhance the potency of the drug and combat drug resistance by promoting cellular uptake, decreasing its efflux and reduce systemic toxicity of the drug [35]. Results obtained in the present investigation demonstrate that the MCP I of *Carica papaya* loaded mPEG-PLA polymeric nanomicelles (MCPI-PNs) opened a new facade of delivery of drug for contraceptive studies.

Polymeric micelles are generally synthesized by direct dissolution using stirring, thermal, or ultrasound treatments. Further, the direct dissolution, solvent evaporation, and dialysis are three usually used methods for drug loading in nanomicelles [36]. In the present study, the ring opening polymerization method of [27] with certain modifications like maintaining the temperature at 130 °C with continuous stirring was followed for the synthesis of mPEG-PLA polymer. The recrystallization and precipitation, respectively, were carried out by dichloromethane and diethyl ether at -20 °C and finally purified the mPEG-PLA copolymer/polymer dried in a vacuum evaporator [37]. The successful synthesis of mPEG-PLA copolymer/polymer took place in the present investigation verified by NMR, linear structure by FTIR and crystalline structure by X-ray diffraction [38,39]. Direct dissolution in 1 mL of Milli-Q water was carried out for loading of MCP I at 5, 15 and 45 µL concentrations. It imparts the 100 – 166 nm sized MCPI-PNs [40, 41]. The determination of size of nanomicelles is commonly analyzed by DLS and further compared by both SEM and TEM observations [36, 39]. The average sizes of empty mPEG-PLA and MCPI-PNs, used in the present investigation, determined by DLS were 46.03 nm and 100-166 nm,

respectively. Whilst, the smooth surfaced and spherical shaped blank and MCP I loaded nanomicelles observed were in the range of 20-70 nm and 50-100 nm, respectively. Also, the spherical morphology exhibited with TEM showed the size in the range of 20-100 nm. The variation in the size obtained by DLS and those from SEM and TEM could be due to the dehydration process during sample preparation of the object. This observation, in the present investigation, is in accordance with the Prabakaran et al. who obtained larger sized folate-conjugated amphiphilic hyperbranched block copolymers by DLS used for tumor-targeted drug delivery and smaller from those of TEM observations [42]. Similar observation was also recorded by other investigators [27, 43-45].

Due to poor aqueous solubility the delivery of non-water-soluble drugs to the target sites are difficult. In the present study, we developed and characterized a mPEG-PLA-based nanomicelle system for MCP I (i.e., MCPI-PNs) delivery. It facilitated systemic delivery of MCP I, composed of long chain molecular weight fatty acids, through a marked increase in the aqueous solubility. The MCPI-PNs not only enhanced the adverse effects on reproductive system, it also reduced the dose level, in comparison to pure drug, probably via increased cellular uptake of drug molecules through blood-testis barrier and improved drug pharmacokinetics [46]. This is in accordance with the investigations of Yuan et al., wherein they demonstrated superior anticancer effects by reduction of IC₅₀ value due to the increased cellular uptake of ABG-PNs [47]. The mPEG-PLA copolymer was selected, in the present study, to encapsulate MCP I due to its high physical stability and low critical micelle concentration value of the copolymer. The varied responses in the present study carried out between different groups in terms of sperm characteristics, fertility and histopathology of testes confirm size and

dose dependent reproductive effects of MCPI-PNs. The optimized MCPI-PNs exhibited a desired particle size (100 nm), enormously reduced dose level (from 10 mg/animal/day of MCP I to 1.5 µg/animal/day of MCPI-PNs), sufficient for systemic delivery, efficient passive targeting ability and physical stability (stable for up to 3 months, study not shown) [27, 47].

In the present investigation, both MCPI-PNs (low dose and mid doses) and intact MCP I exhibited maximal decline in cauda epididymal sperm count with drastic decline of percentage of sperm motility and viability, and enhancement in sperm abnormalities, inhibition of spermatogenesis, pyknosis and eruption of germ cells, and vacuolization in Sertoli cells. These observations are in agreement with similar to earlier studies carried out in different animal models treated with varied crude extracts, partially purified and characterized compounds of the seeds of *Carica papaya* [1, 4, 6, 7, 48-53]. These effects seem to both testicular as well as post-testicular at the level of cauda epididymis as assumed in earlier investigations [7, 51]. The observation of absolute sterility following 30 days of administration of MCP I alone and MCPI-PNs (low dose) treated groups indicate enhanced potency of the DDS developed for MCP I.

The unaltered body and reproductive organs weight of treated rats suggest that the MCPI-PNs do not cause any adverse

effects on general health and reproductive organs of the animals [7, 52].

Despite issues related to various physicochemical properties such as drug stability, entrapment efficiency, critical micelle concentration and *in vitro* cell viability tests have not been carried out in the present investigation for the prepared MCPI-PNs. Thus, the present study can be concluded that the 100 nm sized MCPI-PNs showed maximum effects at conspicuous low dose (1.5 µg/animal/day). A detailed long-term contraceptive study, thus, desired to be conducted in different animal models with particular emphasis on reversibility and toxicity.

ACKNOWLEDGMENTS

The infrastructural facilities provided by the Head, University Department of Zoology, Jaipur are gratefully acknowledged. The University Grants Commission, New Delhi for award of the Senior Research Fellowship to RKD. The characterization studies were carried out at the University Science Instrumentation Centre (USIC), University of Rajasthan, Jaipur, and Malviya National Institute of Technology, Jaipur, Rajasthan, India. The award of NASI Senior Scientist's assignment to NKL is gratefully acknowledged.

CONFLICT OF INTEREST

The authors declare that they have no conflict of interest.

REFERENCES

1. Lohiya NK, Goyal RB "Antifertility investigations on the crude chloroform extract of *Carica papaya* Linn. seeds in male albino rats", *Indian J Exp Biol*, 30 (1992) 1051-1055.
2. Lohiya NK, Pathak N, Mishra PK, Manivannan B, "Reversible contraception with chloroform extract of *Carica papaya* Linn. seeds in male rabbits", *Reprod Toxicol* 13 (1999) 59-66.
3. Lohiya NK, Mishra PK, Pathak N, Manivannan B, Jain SC "Reversible azoospermia by oral administration of the benzene chromatographic fraction of the chloroform extract of the seeds of *Carica papaya* in rabbits", *Adv Contracept* 15 (1999) 141-61.
4. Pathak N, Mishra PK, Manivannan B and Lohiya NK., "Sterility due to inhibition of sperm motility by oral administration of benzene chromatographic fraction of the chloroform extract of the seeds of *Carica papaya* in rats", *Phytomedicine* 7 (2000) 325-333.
5. Ansari AS, Shrivastava S, Goyal S and Lohiya NK., "Observations on chromosomal aberrations following treatment with methanol sub-fraction (MSF) of *Carica papaya* seeds for contraception in albino rats and rabbits", *Int J Pharmacol* 7(6) (2011) 721-725.

6. Lohiya NK, Manivannan B, Mishra PK and Pathak N., “Prospects of developing a plant based male contraceptive pill”, In: Chaudhury SR, Gupta CM, Kamboj VP, editors. Current Status in Fertility Regulation: Indigenous and Modern Approaches. Lucknow: Central Drug Research Institute; (2001) 99-119.
7. Lohiya NK, Mishra PK, Pathak N, Manivannan B and Bhande SS., “Efficacy trial on the purified compounds of the seeds of *Carica papaya* for male contraception in albino rat”, *Reprod Toxicol* 20 (2005) 135-148.
8. Lohiya, NK, Pathak N, Mishra PK and Manivannan B., “Contraceptive evaluation and toxicological study of aqueous extract of the seeds of *Carica papaya* in male rabbits”, *J Ethnopharmacol* 70 (2000) 17-27.
9. Haensler J and Szoka FC Jr., “Polyamidoamine cascade polymers mediate efficient transfection of cells in culture”, *Bioconjug Chem* 4 (1993) 372-379.
10. Kukowska-Latallo JF, Bielinska AU, Johnson J, Spindler R, Tomalia DA and Baker JR., “Efficient transfer of genetic material into mammalian cells using starburst polyamidoamine dendrimers”, *Proc Natl Acad Sci USA* 93 (1996) 4897-4902.
11. Yu T, Liu X, Bolcato-Bellemin AL, Wang Y, Liu C, Erbacher P, Qu F, Rocchi P, Behr JP, Peng L., “An amphiphilic dendrimer for effective delivery of small interfering RNA and gene silencing *in vitro* and *in vivo*”, *Chem Int Ed Engl* 51 (2012) 8478-8484.
12. Liu X, Zhou J, Yu T, Chen C, Cheng Q, Sengupta K, Huang Y, Li H, Liu C, Wang Y, Posocco P, Wang M, Cui Q, Giorgio S, Fermeglia M, Qu F, Pricl S, Shi Y, Liang Z, Rocchi P, Rossi JJ, Peng L., “Adaptive amphiphilic dendrimer-based nanoassemblies as robust and versatile siRNA delivery systems”, *Chem Int Ed Engl* 53 (2014) 11822-11827.
13. Choi JS, Nam K, Park JY, Kim JB, Lee JK, Park JS., “Enhanced transfection efficiency of PAMAM dendrimer by surface modification with L-arginine”, *J Controlled Release* 99 (2004) 445-456.
14. Yang HJ, Cho WG and Park SN., “Stability of oil-in-water nano-emulsions prepared using the phase inversion composition method”, *J Ind Eng Chem* 15 (2009) 331-335.
15. Kang EB, Sharker SM, In I and Park SY., “Pluronic mimicking fluorescent carbon nanoparticles conjugated with doxorubicin via acid-cleavable linkage for tumor-targeted drug delivery and bioimaging”, *J Ind Eng Chem* 43 (2016) 150-157.
16. Pourjavadi A, Tehrani ZM, Shirvani T, Doulabi M and Bumajdad A., “Dendritic multi-walled carbon nanotube with thermoresponsive shells: A good carrier for anticancer drugs”, *J Ind Eng Chem* 35 (2016) 332-340.
17. Kukreja A, Kang B, Kim H-O, Jang E, Son HY, Huh Y-M and Haam S., “Preparation of gold core-mesoporous iron-oxide shell nanoparticles and their application as dual MR/CT contrast agent in human gastric cancer cells”, *J Ind Eng Chem* 48 (2017) 56-65.
18. Lim GH and Choi HJ., “Synthesis of self-assembled rectangular-shaped polyaniline nanotubes and their physical characteristics”, *J Ind Eng Chem* 47 (2017) 51-55.
19. Zhao X, Zou X and Ye L., “Controlled pH-and glucose-responsive drug release behavior of cationic chitosan-based nano-composite hydrogels by using graphene oxide as drug nanocarrier”, *J Ind Eng Chem* 49 (2017) 36-45.
20. Gong J, Chen M, Zheng Y, Wang S and Wang Y., “Polymeric micelles drug delivery system in oncology”, *J. Control. Release* 159 (2012) 312-323.
21. Zhang Y, Huang Y and Li S., “Polymeric Micelles: Nanocarriers for Cancer-Targeted Drug Delivery”, *AAPS Pharm Sci Tech* 15 (2014) 862-871.
22. Yokoyama M., “Polymeric micelles as a new drug carrier system and their required considerations for clinical trials”, *Expert Opin Drug Deliv* 7 (2010) 145-158.
23. Amirmahani N, Mahmoodi NO, Galangash MM, and Ghavidast A., “Advances in nanomicelles for sustained drug delivery”, *J Ind Eng Chem* 55 (2017) 21-34.
24. Li Z, Guo Z, Chu D, Feng H, Zhang J, Zhu L and Li J., “Effectively suppressed angiogenesis-mediated retinoblastoma growth using celastrol nanomicelles”, *Drug Deliv* 27 (2020) 358-366.
25. Márquez-Miranda V, Camarada MB, Araya-Durán I, Varas-Concha I, Almonacid DE, González-Nilo FD., “Biomimetics: From Bioinformatics to Rational Design of Dendrimers as Gene Carriers”, *PLoS ONE* 10(9) (2015) e0138392. <https://doi.org/10.1371/journal.pone.0138392>
26. Committee for the Purpose of Control and Supervision of Experiments on Animals (CPCSEA). Guidelines on the Regulation of Scientific Experiments on Animals, Committee for the Purpose of Control and Supervision of Experiments on Animals (CPCSEA). New Delhi, India: Standard Operating Procedures (SOP) for Institutional Animals Ethics Committee (IAEC), Animal Welfare Division, Ministry of Environment, Forests and Climate Change, Government of India; (2010).
27. Hsiue GH, Lo CL, Lin SJ and Tsai HC., “Stable micelles formed with diblock copolymers of critical micelle concentration copolymer and temperature-sensitive copolymer”, US patent US8299178 B2.

28. Yasugia K, Nagasakia Y, Katoa M and Kataokab K., "Preparation and characterization of polymer micelles from poly (ethylene glycol)-poly (D, L lactide) block copolymers as potential drug carrier", *J Control Release* 62 (1999) 89-100.
29. Zhao H, Liu Z, Park S, Kim SH, Kim JH and Piao L., "Preparation and Characterization of PEG/PLA Multiblock and Triblock Copolymer", *Bull Korean Chem Soc* 33 (2012) 1-5.
30. Giita Silverajah VS, Ibrahim NA, Yunus WMZW, Hassan HA and Woei CB., "A Comparative Study on the Mechanical, Thermal and Morphological Characterization of Poly (lactic acid)/Epoxidized Palm Oil Blend", *Int J Mol Sci* 13 (2012) 5878-5898.
31. Zhao M, Li M, Zhang Z, Gong T and Sun X., "Induction of HIV-1 gag specific immune responses by cationic micelles mediated delivery of gag mRNA", *Drug Deliv* 23 (2015) 2596-2607.
32. Xiaozhou S, Lei L and Weihan H., "Characterization of the spindle morphology nanomicelles assembled from sericin and gelatin", *J Nanomater* 2017 (2017) 1-10.
33. Xue Y, Qian X, Keyu S, Zhijie L, Dong D and Baojian W., "Systemic delivery of the anticancer agent arenobufagin using polymeric nanomicelles", *Int J Nanomedicine* 12 (2017) 4981-4989.
34. WHO. "WHO Laboratory Manual for Examination and Processing of the Human Semen", Ed. 5. WHO Press, Geneva, (2017).
35. Wei T, Chen C, Liu J, Liu C, Posocco P, Liu X, Cheng Q, Huo S, Liang Z, Fermeglia M, Pricl S, Liang XJ, Rocchi P and Peng L., "Anticancer drug nanomicelles formed by self assembling amphiphilic dendrimer to combat cancer drug resistance", *Proc Natl Acad Sci* 112 (2015) 2978-2983.
36. Mourya VK, Inamdar N, Nawale RB and Kulthe SS., "Polymeric micelles: General considerations and their applications", *Ind J Pharm Edu Res* 45(2) (2011) 128-138.
37. Webber SE., "Polymer micelles: An example of self assembling polymers", *J Phys Chem B* 102 (1998) 2618-2626.
38. Kabanov AV, Batrakova EV and Alakhov VY., "Pluronic block copolymers as novel polymer therapeutics for drug and gene delivery", *J Control Release* 82 (2002) 189-212.
39. Ordanini S. and Cellesi F., "Complex polymeric architectures self-assembling in unimolecular micelles: Preparation, characterization and drug nanoencapsulation", *Pharmaceutics* 10(209) (2018) 1-19.
40. Jette KK, Law D, Schmitt EA and Kwon GS., "Preparation and drug loading of poly (ethylene glycol)-block-poly(ϵ -caprolactone) micelles through the evaporation of a cosolvent azeotrope", *Pharm Res* 21 (2004) 1184-91.
41. Gohy JF., "Block copolymer micelles", *Adv Polym Sci* 190 (2005) 65-36.
42. Prabakaran M, Grailer JJ, Pilla S, Steeber DA and Gong SQ., "Folate-conjugated amphiphilic hyperbranched block copolymers based on Boltorn (R.) H40, poly(L-lactide) and poly (ethylene glycol) for tumor-targeted drug delivery", *Biomaterials* 30 (2009) 3009-3019.
43. Yang XQ, Grailer JJ, Pilla S, Steeber DA and Gong SQ., "Tumor-Targeting, pH-Responsive, and Stable Unimolecular Micelles as Drug Nanocarriers for Targeted Cancer Therapy", *Bioconjug Chem* 21 (2010) 496-504.
44. Yang H, Zhao X, Zhang X, Ma L, Wang B, Wei H., "Optimization of bioreducible micelles self-assembled from amphiphilic hyperbranched block copolymers for drug delivery", *J Polym Sci A Polym Chem* 56 (2018) 1383-1394.
45. Zhang X, Zhu T, Miao Y, Zhou L and Zhang W., "Dual responsive doxorubicin loaded nanomicelles for enhanced cancer therapy". *J Nanobiotech* 18(1) (2020) 1-17.
46. Cheng CY and Mruk DD., "The blood-testis barrier and its implications for Male contraception", *Pharmacol Rev* 64 (2012) 16-64.
47. Yuan X, Xie Q, Su K, Li Z, Dong D and Wu B., "Systemic delivery of the anticancer agent arenobufagin using polymeric nanomicelles", *Int. J. Nanomedicine*, 12 (2017) 4981-4989.
48. Lohiya NK, Goyal RB, Jayaprakash D, Sharma S and Kumar M., "Induction of reversible antifertility with a crude ethanol extract of *Carica papaya* seeds in albino male rats", *Int J Pharmacog* 30 (1992) 308-20.
49. Lohiya NK, Goyal RB, Jayaprakash D, Ansari AS and Sharma S., "Antifertility effects of aqueous extract of *Carica papaya* seeds in male rats", *Planta Med* 60 (1994) 400-404.
50. Lohiya NK, Goyal RB, Jayaprakash D, Ansari AS and Srivastava S., "Antifertility effects of *Carica papaya* seeds in male rats", In: Puri CP, Van Look PFA, editors. Current Concepts in Fertility Regulation and Reproduction. New Delhi: Wiley Eastern Ltd. (1994) 177-192.
51. Manivannan B, Mittal R, Goyal S, Ansari AS and Lohiya NK., "Sperm characteristics and testis ultrastructure", *Asian J Androl* 11 (2009) 583-599
52. Lohiya NK, Manivannan B and Garg S., "Toxicological investigations on the methanol sub-fraction of the seeds of *Carica papaya* as a male contraceptive in albino rats", *Reprod Toxicol* 22 (2006) 461-468.
53. Lohiya NK, Manivannan B, Goyal S and Ansari AS., "Sperm motility inhibitory effect of the benzene chromatographic fraction of the chloroform extract of the seeds of *Carica papaya* in langur monkey, *Presbytis entellus entellus*", *Asian J Androl* 10 (2008) 298-306.